ISSN 2070-0482, Mathematical Models and Computer Simulations, 2015, Vol. 7, No. 4, pp. 303–314. © Pleiades Publishing, Ltd., 2015.
Original Russian Text © B.N. Azarenok, A.A. Charakhch'yan, 2014, published in Matematicheskoe Modelirovanie, 2014, Vol. 26, No. 12, pp. 48–64.

One problem on Generating 2D Regular Grids Based on Mappings

B. N. Azarenok† and A. A. Charakhch'yan

Dorodnicyn Computing Center, Russian Academy of Sciences, Moscow, Russia

e-mail: chara@ccas.ru

Received October 10, 2013

Abstract—To study the known problem on generating a regular grid by means of the Winslow method in a rectangular domain with a boundary kink known as a backstep, a high-accuracy numerical method for the inverse harmonic mapping of the unit square onto the domain with a certain mapping of the domain boundaries is developed. The behavior of mapping level lines that enter the point of the boundary kink is studied. Near the kink, the angle between the boundary and the straight line connecting a point on the level line with a point of the boundary kink is found as a function of the coordinate of the point on the level line in the unit square. It is shown that the level line of the mapping is tangent to the boundary at the kink point. Near the kink point the mapping is not quasi-isometric. The regular grid generated according to the intersection points between the level lines connected by straight lines contains a self-intersecting cell that remains when the grid step along the boundary decreases. Based on the universal elliptical equations reproducing any nondegenerate mapping of the parametric rectangle onto a given domain, a simple two-parametric control of the grid nodes in the backstep that makes it possible to effectively control the slope angle of the grid line entering the point of the kink, thereby removing the escape of the grid lines from the domain boundary, is suggested. In the case of a small number of grid points 31×31, the nondegenerate grid is generated by selecting a suitable value of one parameter. If the number of grid nodes is increased by a factor of 8 along both directions (grid size 241×241), the nonconvex cells appear within the domain, which are easily removed by using the variational barrier method. Another possibility to avoid nonconvex cells is to decrease the grid dimension along the second direction (grid size 241×121).

Keywords: structured grids, harmonic mapping, control metric

DOI: 10.1134/S207004821504002X

1. INTRODUCTION

After the sudden death of B.N. Azarenok two papers and their codes were found on his computer, with the help of which the results presented in the papers were obtained. The first paper was devoted to the square inverse harmonic mapping to the rectangle domain with a boundary kink known as the backstep or the corner. In the second paper a procedure for generating grids with the help of a quasi-conform mapping in 2D domain with the corner on the boundary is examined. The second author of the work joined these two papers into one and added new results obtained with the help of the codes written by Azarenok. The code that generates a square mapping into the corner was preliminarily tested for estimating its accuracy. Unfortunately when the two papers were united into one chapter, the paragraph where it was described how to generate a grid with orthogonalizaiton and with the given points crowding near the wind profile's boundary had been excluded, since in this paragraph important details of the method were omitted and the respective code was too difficult to understand. How to generate such grids with the help of a few different procedures is described in the last paper written by Azarenok [1].

Methods for generating regular grids in 2D domains with a curvilinear boundary and the points given on this boundary were developed many years ago. Great progress in this field was made through the work written by A. Winslow in 1967 [2], where he suggested generating grids by a harmonic mapping of the given domain Ω in plane (x, y) onto the unit square Θ in the parametric plane (ξ, η). This mapping is described as follows:

$$\Delta\xi = 0, \quad \Delta\eta = 0, \quad \Delta = \frac{\partial^2}{\partial x^2} + \frac{\partial^2}{\partial y^2}, \quad (x, y) \in \Omega. \tag{1}$$

† Deceased.

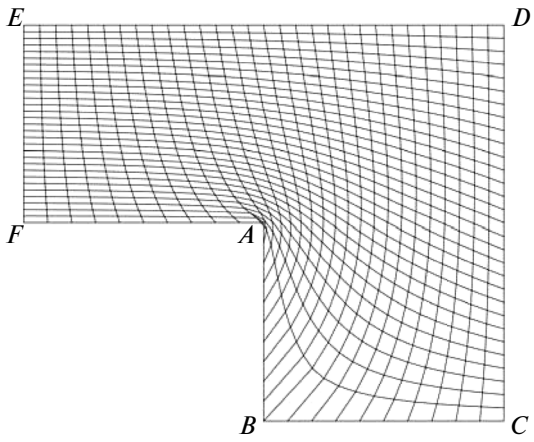

Fig. 1. Domain corner with vertices A, B, C, D, E, F and the 31×31 grid generated by the Winslow method.

Since the mapping procedure is performed into a convex domain (in our case into a square), according to the Radó-Kneser-Choquet theorem [3–5], such a mapping is nondegenerative if the given mapping for domain boundaries is one-to-one. For generating the grid, a rectangular grid in plane (ξ, η) and the points on the boundary of the given domain in plane (x, y) are set and two quasi-linear elliptical equations are solved numerically with respect to functions $x(\xi, \eta)$ and $y(\xi, \eta)$,

$$\mathcal{L}(x) = g_{22}x_{\xi\xi} - 2g_{12}x_{\xi\eta} + g_{11}x_{\eta\eta} = 0, \quad \mathcal{L}(y) = 0,$$
$$g_{11} = x_\xi^2 + y_\xi^2, \quad g_{12} = x_\xi x_\eta + y_\xi y_\eta, \quad g_{22} = x_\eta^2 + y_\eta^2, \tag{2}$$

which are obtained by inverting the variables in Eqs. (10). In the present work, the procedures for approximating Eqs. (2) and their solution are taken from [6]. As a rule, the Winslow method gives nondegenerative grids free of self-intersections. Nevertheless, in several domains, in particular, in the domain which is examined in the present work, this method gives a degenerative grid.

In 1987 S.A. Ivanenko suggested a procedure [7] guaranteeing that the grid was not degenerative. The grid is generated by means of unconditional minimization of a finite function of barrier type that approximates a functional, whose minimum is reached at a solution of the quasi-linear equations of the Winslow method. The price for the method's reliability is computation intensity, which rises by a factor of 10 with the Winslow method. Ivanenko [8] and Azarenok [9] developed a way for generating 2D and 3D adaptive grids by minimizing finite dimensional functions of the barrier type.

Let us point out work [10], published in 2002, where it is shown that a set of functionals which were used earlier for obtaining finite-dimensional functions of the barrier type, determine all possible square nondegenerative mappings onto the given domain in a parametric plane. The respective set of finite-dimensional functions is characterized by the same property. Any nondegenerative grid can be generated by minimizing a function belonging to the set.

G.P. Prokopov who read Ivanenko's manuscript was the first person who understood how Ivanenko's work was important for developing the alternative procedures for generating grids without minimizing barrier functions. In 2001 Prokopov published a work where he presented the results obtained by Ivanenko and showed that the set of functionals [12] free of the Jacobian mapping in the integrand denominator was characterized by the same property. The respective finite-dimensional functions have no barrier securing the grid's nondegeneracy, but its set is characterized by the same property: to reproduce any nondegenerative grid. In this way, the problem of generating a nondegenerative grid is reduced to the problem of determining suitable metric coefficients, which determine the required set function. [13–15] are a continuation of these works.

Azarenok found another way for developing reliable procedures for generating grids without minimizing barrier functions. He used the idea that the revealed by Ivanenko property of the set of functionals is transported obviously to the set of Euler equations. In this case it is possible to use any approximation of Euler equations, i.e., to return to the idea of Winslow method, and to use it for more complicated quasi-linear equations, and to secure a grid's nondegeneracy by searching for the proper coefficients in these equations.

The first step on the way to developing such a procedure is to examine all known examples in which the degenerative grid is generated by the Winslow method. In the first work devoted to this problem [16], the known example [17] on generating improper grids by the Winslow method in a horseshoe-shaped domain is examined. The second work is work [1] cited above. The presented work continues this cycle.

The examined domain, which we call the corner, is a hexagon in the form of a square with a quarter cut out (see Fig. 1). In this domain a regular grid consisting of two sets of lines needs to be generated. The lines of the first set connect the boundary points on the straight line ED and polygonal line $FABC$. The lines of the second set connect the boundary points on lines EF and DC.

Figure 1 depicts the 31×31 grid generated by the Winslow method. The points along all the boundaries are placed uniformly. It is seen that near vertex A there is a self-intersecting cell. The degeneration of such a grid for the examined domain was known long ago [18].

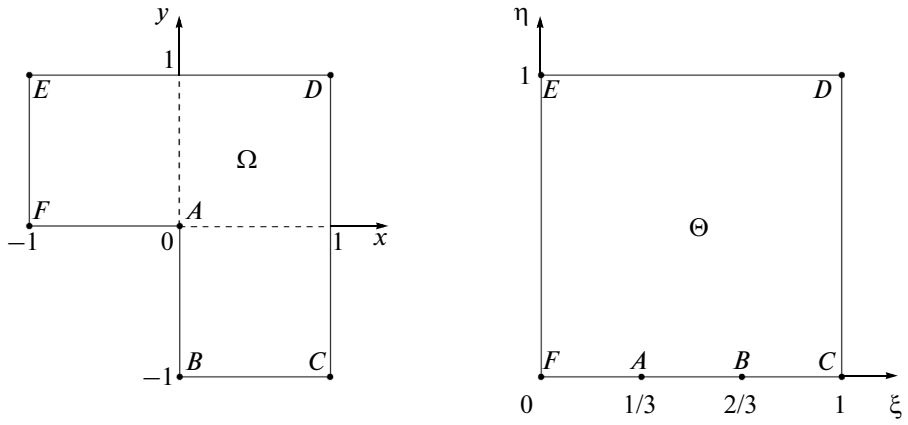

Fig. 2. The correlation between the boundary of corner Ω in plane (x, y) and the unit tetragon Θ in plane (ξ, η).

The grid in Fig. 1 is generated by solving Eq. (2) numerically for a square grid in domain Θ with step $h = 1/N$, $N = 30$ for both variables ξ and η. Since the exact solution of Eq. (2) is a non degenerative mapping, it is reasonable to assume that under $N \to \infty$, grid degeneracy should be avoided. Ivanenko was the first person who showed that it was not the case. He performed calculations for embedded grids and saw that the form of the self-intersecting cell near point A became worse if the number of points increased.

The present work consists of two main sections. In Section 2, a highly accurate method for calculating inverse harmonic mapping of the unit square onto a corner free of the numerical solution of Eq. (2) is developed. The investigation performed with its help makes it possible to understand why a grid's degeneracy generated by solving Eq. (2) numerically cannot be avoided by refining the grid's step in the unit square Θ. In Section 3 we suggest a simple way of controlling the grid's line entering point A, which makes it possible to generate proper grids.

2. INVERSE HARMONIC MAPPING OF A UNIT SQUARE ONTO A CORNER

Let us examine the harmonic mapping $\xi = \xi(x, y)$, $\eta = \eta(x, y)$ of corner Ω onto unit square Θ. We write the boundary conditions for Eqs. (1)

$$\xi = \xi_b(x, y), \quad \eta = \eta_b(x, y), \quad (x, y) \in \partial\Omega, \tag{3}$$

by linearly mapping each side of corner Ω onto the respective segment lying on the side of square Θ (see. Fig. 2). Let us examine the case when side FC of square Θ is separated into three equal parts by points A and B. The boundary conditions can be written as follows:

$$\begin{gathered} FA\colon\ \xi = \frac{1}{3}(1+x),\ \ \eta = 0,\ \ -1 \le x \le 0,\ \ CD\colon\ \xi = 1,\ \ \eta = \frac{1}{2}(1+y),\ \ -1 \le y \le 1, \\ AB\colon\ \xi = \frac{1}{3}(1-y),\ \ \eta = 0,\ \ -1 \le y \le 0,\ \ DE\colon\ \xi = \frac{1}{2}(1+x),\ \ \eta = 1,\ \ -1 \le x \le 1, \\ BC\colon\ \xi = \frac{1}{3}(2+x),\ \ \eta = 0,\ \ 0 \le x \le 1,\ \ EF\colon\ \xi = 0,\ \ \eta = y,\ \ 0 \le y \le 1. \end{gathered} \tag{4}$$

Let there be a conform mapping $r = r(x, y)$, $\varphi = \varphi(x, y)$ of corner Ω in the complex plane $z = x + iy$ onto unit circle $\mathbb{D}$ in the complex plane $z_1 = x_1 + iy_1 = r\exp(i\varphi)$, $0 \le r \le 1$, $0 \le \varphi < 2\pi$ and the inverse mapping $x = x(r, \varphi)$, $y = y(r, \varphi)$, which is also conform. In this case functions $\tilde{\xi}(r, \varphi) = \xi(x(r, \varphi), y(r, \varphi))$ and $\tilde{\eta}(r, \varphi) = \eta(x(r, \varphi), y(r, \varphi))$ are harmonic in the unit circle $\mathbb{D}$ (since functions $\xi = \xi(x, y)$, $\eta = \eta(x, y)$ are harmonic) and are determined by the Poisson integral

$$\tilde{\xi}(r, \varphi) = \frac{1}{2\pi}\int_0^{2\pi} \tilde{\xi}(1, t)\frac{1 - r^2}{1 - 2r\cos(t - \varphi) + r^2}\,dt, \quad \tilde{\eta}(r, \varphi) = \frac{1}{2\pi}\int_0^{2\pi} \tilde{\eta}(1, t)\frac{1 - r^2}{1 - 2r\cos(t - \varphi) + r^2}\,dt. \tag{5}$$

Functions on the circle's boundaries are determined by the given functions (3) on the corner's boundary: $\tilde{\xi}(1, \varphi) = \xi_b(x(1, \varphi), y(1, \varphi))$ and $\tilde{\eta}(1, \varphi) = \eta_b(x(1, \varphi), y(1, \varphi))$.

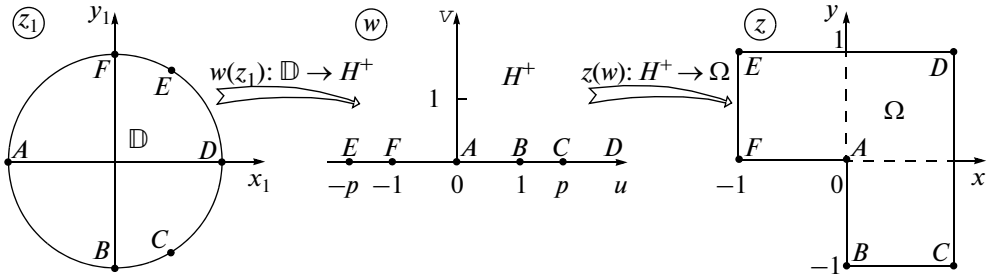

Fig. 3. Block-diagram for generating the conform mapping of a unit circle onto the corner

The unknown inverse harmonic mapping $x = x(\xi, \eta)$, $y = y(\xi, \eta)$ is generated in the following way. The square's boundaries are mapped easily onto the corner's boundary by inversing functions (4). Now let a certain point (ξ, η) be set and it is not on the square's boundary. First of all we solve the following equations by Newton's method

$$\tilde{\xi}(r, \varphi) = \xi, \quad \tilde{\eta}(r, \varphi) = \eta, \tag{6}$$

and after that the unknown values x and y are determined by conform mapping $x = x(r, \varphi)$ and $y = y(r, \varphi)$.

The derivatives needed for Newton method $\tilde{\xi}_r$, $\tilde{\xi}_\varphi$, $\tilde{\eta}_r$, $\tilde{\eta}_\varphi$ are determined by differentiating Eqs. (5). For example, for $\tilde{\xi}_r$, $\tilde{\xi}_\varphi$, we have

$$\frac{\partial \tilde{\xi}}{\partial r} = \frac{1}{2\pi} \int_0^{2\pi} \tilde{\xi}(1, t) \frac{-2[rg + (r - \cos(t - \varphi))f]}{g^2} dt, \quad \frac{\partial \tilde{\xi}}{\partial \varphi} = \frac{1}{2\pi} \int_0^{2\pi} \tilde{\xi}(1, t) \frac{2rf \sin(t - \varphi)}{g^2} dt, \tag{7}$$

where $f = 1 - r^2$ and $g = 1 - 2r\cos(t - \varphi) + r^2$. The iteration in the Newton method is performed until the following conditions become true $\left| z_1^{l+1} - z_1^l \right| \le 10^{-10}$, where l is the number of iteration and $z_1^l = r_l \exp(i\varphi_l)$.

Newton's method for Eq. (6) requires setting the initial values for r and φ under which this method converges. The presented algorithm is used for generating the mapping level lines $x = x(\xi, \eta)$ and $y = y(\xi, \eta)$. The first point of the level line is chosen near a certain point (ξ_b, η_b) of the square's boundary. The initial value for r is chosen near 1, and the initial value for φ is determined by conform mapping $\varphi = \varphi(x_b, y_b)$ of the respective point on the corner's boundary. After that the level lines are generated by varying a few of the coordinates. The initial approximations for r and φ are taken from the calculation for the previous point.

Poisson integral (5) and its derivatives are calculated by using Simpson's formula according to the angular coordinate φ of the grid consisting of 10^5 points.

2.1. Conform mapping of a unit circle onto a corner. The unknown conform mapping $z(z_1)$ we determine (see Fig. 3) in the form of a composition of a linear-fractional mapping of unit circle $\mathbb{D}$ onto the upper semi-plane H^+ of complex plane $w = u + iv$

$$w(z_1) = i\frac{1 + z_1}{1 - z_1} \tag{8}$$

and mapping H^+ to Ω, which is presented by the Christoffel-Schwartz integral (see, for example, [20]) under the given correspondence between three points $F(-1, 0)$, $A(0, 0)$, and $B(1, 0)$ from H^+ and three points on $\partial\Omega$

$$z(w) = K \int_0^w \zeta^{\alpha_A - 1}(\zeta - 1)^{\alpha_B - 1}(\zeta - p)^{\alpha_C - 1}(\zeta + 1)^{\alpha_F - 1}(\zeta + p)^{\alpha_E - 1} d\zeta,$$

where K is a complex constant, $\pm p$ are coordinates of the preimages of vertices C and E of corner Ω (according to Schwartz's symmetry principal points $-p$ and -1 on axis u are the preimages of vertices C and F of corner Ω). The infinitely distant point on H^+ corresponds to vertex D. Parameters α_i are determined by the internal angles of corner vertexes $\psi_i = \pi\alpha_i$, from which $\alpha_A = 3/2$, $\alpha_B = \alpha_C = \alpha_F = \alpha_E = 1/2$. Function $z(w)$ can be written as follows:

$$z(w) = K\int_0^w \zeta^{1/2}(\zeta^2 - 1)^{-1/2}(\zeta^2 - p^2)^{-1/2}d\zeta. \tag{9}$$

If integral (9) is used, it is necessary to determine preliminary parameters p and K needed for calculating improper integrals. In the present work these integrals are calculated with the help of a hypergeometric function [21]. Let us change variables $s = u^2$ in (9) under integration along the real axis $u = \mathrm{Re}\,\zeta > 0$. As a result we have

$$\begin{gathered} z(1) = -\frac{K}{2p}I_0^1, \quad |AB| = \frac{|K|}{2p}I_0^1, \quad I_0^1 = \int_0^1 s^{-1/4}(1-s)^{-1/2}\left(1-\frac{s}{p^2}\right)^{-1/2} ds, \\ |BC| = \frac{|K|}{2p}I_1^{p^2}, \quad I_1^{p^2} = \int_1^{p^2} s^{-1/4}(s-1)^{-1/2}\left(1-\frac{s}{p^2}\right)^{-1/2} ds, \end{gathered} \tag{10}$$

where $|AB|$ and $|BC|$ are the respective sides' lengths of corner Ω.

Let us write the first integral in (10) as follows:

$$I_0^1 = \int_0^1 s^{\beta_0 - 1}(1-s)^{\gamma_0 - \beta_0 - 1}\left(1-\frac{s}{p^2}\right)^{-\alpha_0} ds = \frac{\Gamma(\beta_0)\Gamma(\gamma_0 - \beta_0)}{\Gamma(\gamma_0)}F(\alpha_0, \beta_0, \gamma_0;\, 1/p^2),$$

$$\alpha_0 = \frac{1}{2}, \quad \beta_0 = \frac{3}{4}, \quad \gamma_0 = \frac{5}{4},$$

where $F(\alpha_0, \beta_0, \gamma_0;\, 1/p^2)$ is the hypergeometric function; and $\Gamma\left(\frac{3}{4}\right) = 1.225416702$, $\Gamma\left(\frac{5}{4}\right) = 0.906402477$, and $\Gamma\left(\frac{1}{2}\right) = \sqrt{\pi}$ are the values of the gamma-function presented in [22].

If we present $F(\alpha_0, \beta_0, \gamma_0;\, 1/p^2)$ in the form of a hypergeometric series [23], we have

$$I_0^1 = \frac{\Gamma(\beta_0)\Gamma(\gamma_0 - \beta_0)}{\Gamma(\gamma_0)}\sum_{n=0}^{\infty}\frac{(\alpha_0)_n(\beta_0)_n}{(\gamma_0)_n\, n!}\, p^{-2n}, \tag{11}$$

where $(\alpha_0)_n = \alpha_0(\alpha_0 + 1)\cdots(\alpha_0 + n - 1)$ is Pochhammer's symbol. Series (11) converges under $p > 1$.

The second integral in (10) after substituting $s = 1 + t(p^2 - 1)$ can be written as follows:

$$I_1^{p^2} = p\int_0^1 t^{-1/2}(1-t)^{-1/2}(1-qt)^{-1/4}dt = p\frac{\Gamma(\beta_1)\Gamma(\gamma_1 - \beta_1)}{\Gamma(\gamma_1)}F(\alpha_1, \beta_1, \gamma_1; q),$$

$$q = 1 - p^2, \quad \alpha_1 = \frac{1}{4}, \quad \beta_1 = \frac{1}{2}, \quad \gamma_1 = 1.$$

Since $\Gamma(1/2) = \sqrt{\pi}$, $\Gamma(1) = 1$ and $(\gamma_1)_n = (1)_n = n!$, we have

$$I_1^{p^2} = p\pi\sum_{n=0}^{\infty}\frac{(\alpha_1)_n(\beta_1)_n}{(n!)^2}(1-p^2)^n. \tag{12}$$

Series (12) converges under $|1 - p^2| < 1$. Summarizing the procedure for the series in (11) and (12) is finished when the magnitude of next term of the series becomes lower than 10^{-15}.

Parameter p is determined from condition $|AB|/|BC| = 1$. The respective equation can be written as $I_1^{p^2} - I_0^1 = 0$. If we solve it by Newton's method with initial value $p_0 = 1.1$, we obtain that $p = 1.154700545$. Constant K is determined from condition $z(1) = -i$ (see Fig. 3) and according to (10) $K = 2ip/I_0^1 = 0.660569333i$.

It is sufficient to calculate integral (9) for $u = \mathrm{Re}w \geq 0$, and for $u < 0$ we can use the symmetry condition $x(u, v) = y(-u, v)$, $y(u, v) = x(-u, v)$. The integration procedure until a certain point $w = u + iv$ is performed at first along the real axis up to value u, and after that along the imaginary axis up to value v. At points

$u = 1$, p the integrand in (9) is equal to infinity. For calculating this integral let us separate the right quadrant of the upper semi-plane H^+ into 3 domains.

Formula (9) is used in the semistripe $0 \le \mathrm{Re}\zeta < 1$. In the semistripe $1 \le \mathrm{Re}\zeta < p$ Eq. (9) can be written as follows with the help of change of variables $t = \sqrt{\zeta^2 - 1}$

$$z(w) = z_B + K\int_0^T (1+t^2)^{-1/4}(1+t^2-p^2)^{-1/2}dt, \quad z_B = -i, \quad T = \sqrt{w^2-1}. \tag{13}$$

For $\mathrm{Re}\zeta \ge p$ by substituting variables $t = \sqrt{\zeta^2 - p^2}$ formula (9) can be written as

$$z(w) = z_C + K\int_0^T (t^2+p^2)^{-1/4}(t^2+p^2-1)^{-1/2}dt, \quad z_C = 1-i, \quad T = \sqrt{w^2-p^2}. \tag{14}$$

Strictly speaking, formulas (9), (13), and (14) do not eliminate the integrant's peculiarities. For example, the integrant in (9) goes to infinity under $\zeta \to 1$, $\zeta < 1$. To eliminate this peculiarity it is necessary to do as follows [24]: each integration domain should be separated by an intermediate point into two subdomains with its own change of variables, which makes it possible to eliminate the peculiarity on the respective domain's boundary. However, the formulas presented above, which allow us to formally eliminate the peculiarity only on one end of the domain, make it possible to perform the abend-free calculation with modern computers. If we use the standard doubly-accurate data of 8 bytes, "infinity" is a value higher than 10^{300}. For this purpose the integrant in (9) should be calculated at point $1-d$, where $0 < d < 10^{-600}$, which is impossible since the accuracy of the number presentation for such data is approximately up to 20 decimal digits, not several hundreds.

To estimate the accuracy of the calculation according to formula (9) for the grids which are used in the presented work (see below), we perform several calculations for real values $w = 1-d$, $0 < d \le 10^{-17}$. The results are compared with the calculations obtained by introducing the intermediate point $\zeta_* = 0.5$ and by changing variables $t = (1-\zeta^2)^{1/2}$ in the segment $0.5 \le \zeta \le d$, which make it possible to eliminate the integrant peculiarity under $\zeta = 1$. Under $d = 10^{-7}$ the relative error of formula (9) is $\delta \approx 10^{-5}$. If d is reduced, error δ increases, and under $d = 10^{-16}$, the integral calculated according to formula (9) is higher approximately by a factor of 6 than the exact value. If $d = 10^{-17}$, the computer value of $1-d$ coincides with 1 and the calculation should be repeated according to formula (13), which gives the proper result.

The presented work aims to generate the mapping level lines $x = x(\xi,\eta)$ and $y = y(\xi,\eta)$; the small interval $1-10^{-7} < \mathrm{Re}\, w < 1$, where the accuracy can drop significantly, and approximately the same interval near point $w = p$ are not important since the only vertex of domain Ω in which the level line enters is vertex A. Its image in plane w is point $w = 0$, where the integrant in (9) has no peculiarity.

Note that the Poisson integral (5) and its derivatives (7) are calculated for a grid consisting of 10^5 points placed uniformly (along the arc) along the unit circle in plane z_1 (see Fig. 3). The procedure for generating mapping level lines $x = x(\xi,\eta)$ and $y = y(\xi,\eta)$ starts from the preliminary stage at which the point images are determined. First of all according to formula (8), points u_i, $i = 1,2,\ldots,10^5$ are determined along the real axis of plane w and after that according to formulas (9), (13), and (14), points $(x,y)_i$ are determined on the boundary of corner Ω and after that according to formulas (4), points $(\xi,\eta)_i$ are determined on the boundary of unit square Θ. Integrals for segments $[u_k, u_{k+1}]$ in (9), (13), and (14) are calculated for a uinform grid consisting of 100 points.

For determining image (x,y) of point (ξ,η), which does not belong to the boundary of the unit square, first of all the Poison integral (5) is inversed and point (r,φ) is determined on the unit circle, after that according to formula (8), point (u,v), $v > 0$ is determined on the upper semi-plane H^+, and after that according to formulas (9), (13), and (14), the unknown point (x, y) is found. When we integrate (9), (13), and (14) along the real axis, points u_i, whose images have already been determined, are used. If $u_k < u < u_{k+1}$, the integral is calculated along segment $[(u_k,0),(u,0)]$, which is separated into 100 equal parts. After that the integration is performed along segment $[(u,0),(u,v)]$, which is separated into 10^4 equal parts. In all cases the numerical integration is performed with the help of Simpson's formula.

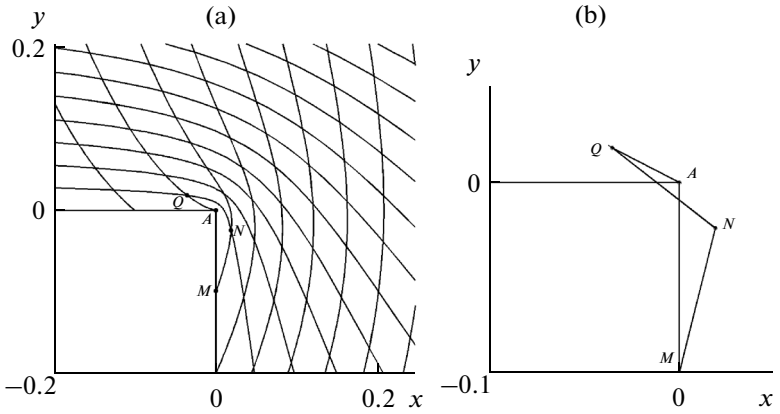

Fig. 4. A fragment of level line mapping in the vicinity of vertex A (a) and cell $AMNQ$ of the grid generated according to level line points of intersection with the help of straight lines (b).

2.2. The calculation results. For testing the code, it was modified for calculations with the doubly-accurate data of 16 bytes. This makes it possible to calculate the first and second derivatives for functions $x(\xi,\eta)$ and $y(\xi,\eta)$ by means of numerical differentiation, for example, $x_\xi = [x(\xi + h_\xi) - x(\xi - h_\xi)]/2h_\xi$ with a very small step $h_\xi = h_\eta = 10^{-8}$. The derivatives calculated with such a procedure are substituted in Eqs. (2) and the misalignment of these equations is calculated. The relative misalignment is determined by dividing into the maximal (over magnitude) summand entering into the equation. With the exception of a small vicinity of the unit square's boundary with a width of approximately 10^{-4}, the maximal relative misalignment is 10^{-4} or lower and it means that the procedure is suitable for investigating mapping properties since functions $x(\xi,\eta)$ and $y(\xi,\eta)$ are set on the boundary. The relative error near the boundary rises since the integrant of Poison integral (5) degenerates into a δ-function at the unit circle.

Figure 4a depicts a fragment of level lines mapping $x = x(\xi,\eta)$ and $y = y(\xi,\eta)$ in the vicinity of the corner's vertex A, which are obtained by the square grid's mapping in the unit square Θ with a step of $h = 1/30$ along both directions. The intersection points of the level lines are the grid nodes. The vertices of curvilinear quadrilateral $AMNQ$ (one of them is the corner's vertex) are marked.

As a rule the grid's neighboring nodes, which are connected by the straight lines, are used for approximating the equations of mathematical physics. Formally we can accept that the level lines in Fig. 4a are in the form of a grid. However, its usage makes it difficult to generate approximating algebraic equations, which depend on the level lines' shape and it becomes impossible to use the developed application packages.

If we connect the grid's nodes in Fig. 4a by straight lines, the curvilinear quadrilateral $AMNQ$ transforms into the self-intersecting cell presented in Fig. 4b. The reason for this phenomenon is the behavior of level line $\xi = \xi_A = 1/3$ leaving point A. Looking at Fig. 4a it s possible to assume that at vertex A this level line is tangential to the corner's boundary $y = 0$. We investigate the properties of level line $\xi = \xi_A$ near vertex A and the results of the investigation confirm this assumption.

Figure 5 depicts the ratio x/η and the logarithm of $y/|x|$ as functions of logarithm η along level line $\xi = \xi_A$ for small values $10^{-4} \le \eta \le 10^{-2}$. For all points in Fig. 5 the relative misalignment for Eqs. (2) is lower than 2×10^{-5}. As it is seen from the first function, $x/\eta \to \text{const}$ under $\eta \to 0$. The second function is a straight line (with a high degree of accuracy) and therefore $y/|x| = c\eta^a$, $c \approx 1.5$ and $a \approx 0.35$. Since $a > 0$, $y/|x| \to 0$ under $\eta \to 0$ and it means that the level line is tangential to the boundary at point $x = 0$, $y = 0$.

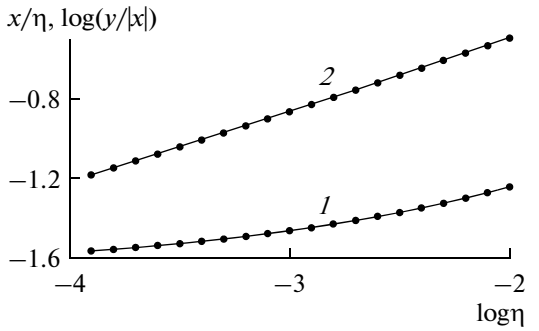

Fig. 5. The ratio x/η (1) and $\log(y/|x|)$ (2) against $\log\eta$ along the level line $\xi = \xi_A$.

The degree of degeneracy σ for cell $AMNQ$ under different $h = 1/(30N)$

N	1	2	4	8	16	32	64	128	256
σ	0.37	0.44	0.5	0.54	0.58	0.61	0.63	0.65	0.66

The examined mapping is not quasi-isometric in the vicinity of vertex A. Let us show that the ratio of the distance d_{xy} between the two points in Ω and the distance $d_{\xi\eta}$ between their preimages in Θ can be arbitrarily small. Let us take point (x, y) on the level line $\xi = \xi_A$ and point $(x, 0)$ on the boundary. Their preimages are points (ξ_A, η) and $(\xi, 0)$, respectively. In this case $d_{xy} = y$, $d_{\xi\eta} = [(\xi - \xi_A)^2 + \eta^2]^{1/2}$. The boundary condition (3) gives $\xi - \xi_A = x/3$ and from here

$$\frac{d_{xy}}{d_{\xi\eta}} = \frac{y}{[x^2/9 + \eta^2]^{1/2}} < 3\frac{y}{|x|} \to 0 \text{ for } \eta \to 0.$$

The level line $\xi = \xi_A$ is tangential to the corner's boundary and therefore, the self-intersecting cell of the grid does not disappear under $h \to 0$. To be convinced of this fact we calculate the vertices of cell $AMNQ$ in Fig. 4b under decreasing h. The following value is chosen as the degree of degeneracy: $\sigma = \sum_{s_k<0}|s_k| \Big/ \sum_{k=1}^{4}|s_k|$, where s_k, $k = 1,2,3,4$ are the squares of four triangles at the cell's vertices. The summarizing procedure in the numerator is performed for triangles with negative squares. For the convex cell $\sigma = 0$. If $s = 0.5\sum_{k=1}^{4} s_k < 0$, then $\sigma > 0.5$.

The results of the calculations are presented in the table for h, which decreases step-by-step by a factor of two. It is seen that the degree of degeneracy increases if h is decreased as revealed by Ivanenko [19], when he calculated grids by the Winslow method. For all h the condition of a cell's self-intersection [25] is true: $s_1 s_3 \le 0$ and $s_2 s_4 \le 0$. Such degeneration of a grid's cell takes place if we use any highly accurate method for Laplace Eq. (1), for example, multipole method [26].

3. THE WAY TO GENERATE A NON DEGENERATIVE GRID IN THE CORNER

For generation we use a set of elliptical differential equations [16]

$$\begin{gathered}\tilde{\mathcal{L}}(x) = \mathcal{L}(x) - x_\xi[\tilde{G}_{22}(P - Q) + \tilde{G}_{12}(S - R)] \\ - x_\eta[\tilde{G}_{11}(R - S) + \tilde{G}_{12}(Q - P)] = 0, \quad \tilde{\mathcal{L}}(y) = 0, \\ P = g_{11}\frac{\partial \tilde{G}_{12}}{\partial \eta} - g_{12}\frac{\partial \tilde{G}_{11}}{\partial \eta}, \quad Q = \frac{1}{2}\left(g_{11}\frac{\partial \tilde{G}_{22}}{\partial \xi} - g_{22}\frac{\partial \tilde{G}_{11}}{\partial \xi}\right), \\ S = g_{12}\frac{\partial \tilde{G}_{22}}{\partial \xi} - g_{22}\frac{\partial \tilde{G}_{12}}{\partial \xi}, \quad R = \frac{1}{2}\left(g_{11}\frac{\partial \tilde{G}_{22}}{\partial \eta} - g_{22}\frac{\partial \tilde{G}_{11}}{\partial \eta}\right),\end{gathered} \tag{15}$$

where $\mathcal{L}(\cdot)$ is the operator from set (2) and $\tilde{G}_{kl}$ is a tensor of normalized metric coefficients of additional mapping $X = X(\xi, \eta)$, $Y = Y(\xi, \eta)$:

$$G_{11} = X_\xi^2 + Y_\xi^2, \quad G_{12} = X_\xi X_\eta + Y_\xi Y_\eta, \quad G_{22} = X_\eta^2 + Y_\eta^2,$$

$$\tilde{G}_{kl} = G_{kl}/\sqrt{\det G}, \quad k,l = 1,2, \quad \sqrt{\det G} = \sqrt{G_{11}G_{22} - G_{12}^2} = X_\xi Y_\eta + X_\eta Y_\xi.$$

Set (15) represents the Euler functional suggested in [27] for grid generation. As the functional itself (see [10, 11]), Eqs. (15) are universal ones since they make it possible to reproduce any smooth geomorphic mapping by setting its metric tensor as a control tensor G_{kl} [16].

If the controlling tensor G_{kl} is generated according to mapping $X(\xi, \eta)$ and $Y(\xi, \eta)$, which is not a mapping of the parametric domain to the given domain in plane (x, y), such a mapping does not coincide with the solution for Eq. (15). Nevertheless, we can hope that certain properties of the control mapping will be intrinsic to the solution of Eq. (15).

If G_{kl} is the unit tensor, Eqs. (15) coincide with (2). It allows us to vary the grid generated according to Eq. (2) only in those domains where it is necessary.

Since Eqs. (15) are invariant with respect to multiplication for independent variables ξ and η on to the same number, the finite-difference approximation of these equations on the square grid gives algebraic

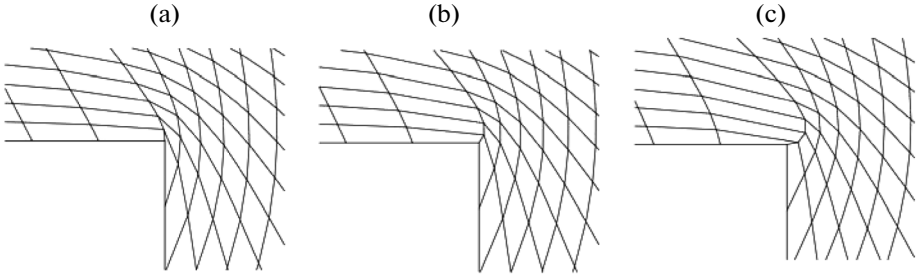

Fig. 6. Fragment of a 31×31 grid for $p = 0.81$ (a), 0.77 (b) and 0.74 (c).

equations independent of the grid's step. That is why it is convenient to approximate Eqs. (15) at the square grid with step 1 by presenting the coordinates of the grid lines in plane (ξ, η) with the help of integer numbers coinciding with the nodes' numeration in the plane (x, y).

For definiteness let us assume that in vertex A $i = \xi = 0$. If we want to prevent the grid's lines going beyond the domain, as is the case if we use Eqs. (2), it is necessary to change the inclination of the grid's line $i = 0$ in the vicinity of point A. As seen from Fig. 4, we can try to obtain the required effect by bring the nodes of line $i = 0$ closer to the nodes of line $i = 1$ near the bottom boundary of the domain.

Let us examine the following mapping:

$$X = X(\xi), \quad Y = \eta, \tag{16}$$

with the controlling tensor components of $G_{11} = X_\xi^2$, $G_{12} = 0$, $G_{22} = 1$ and with the Jacobian $\sqrt{\det G} = X_\xi$. The components of the normalized tensor $\tilde{G}_{kl} = G_{kl}/\sqrt{\det G}$ and their derivatives can be written as follows:

$$\begin{gathered} \tilde{G}_{11} = X_\xi, \quad \tilde{G}_{22} = 1/X_\xi, \\ (\tilde{G}_{11})_\xi = X_{\xi\xi}, \quad (\tilde{G}_{11})_\eta = 0, \quad (\tilde{G}_{22})_\xi = -X_{\xi\xi}/X_\xi^2, \quad (\tilde{G}_{22})_\eta = 0. \end{gathered} \tag{17}$$

If we set function $X(\xi)$ at three points $X(-1) = -1$, $X(0) = 0$, and $X(1) = p$, where $p < 1$ is a parameter, we obtain the mapping which reduces the distance between images for points $\xi = 1$ and $\xi = 0$ with respect to the distance between the images for points $\xi = -1$ and $\xi = 0$. Let $X(\xi)$ be a polynomial of the second order $X(\xi) = a\xi^2 + b\xi + c$, in this case we have $a = 0.5(p-1)$, $b = 0.5(p+1)$, $c = 0$ and at point $\xi = 0$

$$X_\xi = 0.5(p+1), \quad X_{\xi\xi} = p - 1. \tag{18}$$

Let us determine the controlling tensor $\tilde{G}_{kl}$ by formulas (17) and (18) with the same value of parameter p for the nodes of the grid's line $i = 0$, $j = 2, 3, \ldots, j_0$, where $j = 1$ corresponds to the corner's vertex A. At the other nodes, $\tilde{G}_{kl}$ is the unit tensor, which corresponds to $p = 1$ in formulas (17) and (18). In this way the grid's nodes are controlled with the help of two parameters p and j_0. For all the results presented below $j_0 = 7$.

Strictly speaking, tensor $\tilde{G}_{kl}$ chosen with the help of such a procedure is not determined by mapping (16), for which it is accepted that parameter p is independent of η and therefore, of index j. Mapping (16) can be examined as a leading idea for determining the two-parametric set of controlling tensors.

The grids' fragments 31×31 are presented in Fig. 6 for three p values. It is seen that by varying parameter p it is possible to efficiently control the incidental angle of the grid's line $i = 0$ with respect to the boundary and as a result to prevent the grid's lines going beyond the boundary (see Fig. 1) in the absence of control. Further experiments with an increased number of the grid's nodes are performed for $p = 0.77$. The respective grid 31×31, whose fragment is presented in Fig. 6b, consists only of convex cells.

If the number of the grid's nodes is doubled along each direction (grid 61×61), its cells remain convex tetragons. If we again double the number of nodes (grid 121×121), the grid's lines are still within the corner's boundaries, but near vertex A internal cells that are not convex appear. If the number of nodes is increased further (grid 241×241), this grid's defect becomes stronger (see Fig. 7a). Let us point out that the cells that are not convex can be used for the calculations in contrast to the self-intersecting ones (see [25]).

We can try to get rid of the cells that are not convex by changing the ratio between the number of nodes over indices i and j and choosing a more suitable value of parameter p. The results for grid 241×121 and

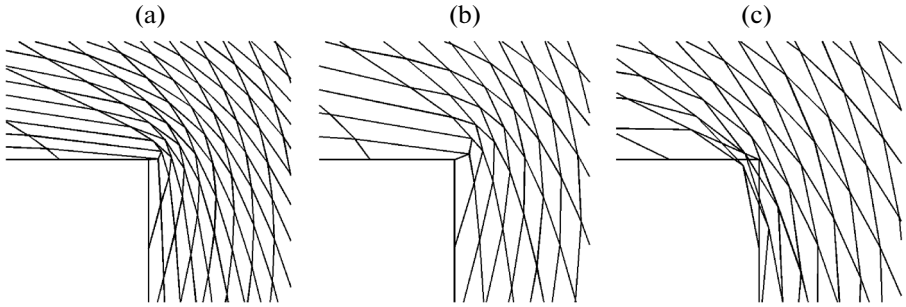

Fig. 7. Fragment of a 241 × 241 grid for $p = 0.77$ (a) and of a 241 × 241 grid for $p = 0.65$ (b) and $p=1$ (c) (standard Winslow method).

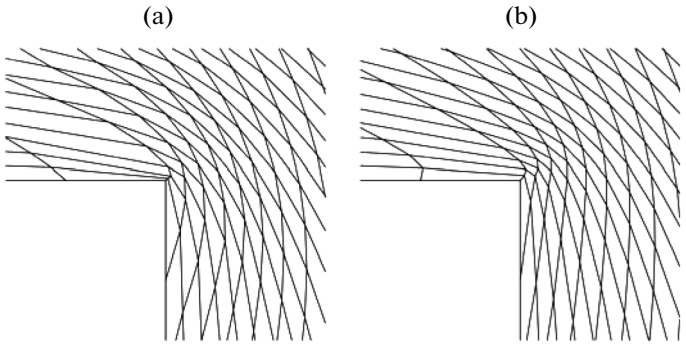

Fig. 8. Fragment of the 241 × 241 grid generated from the grid for $p = 0.77$ after the preliminary stage of the variational barrier method (a) and after the main stage (b).

$p = 0.65$ presented in Fig. 7b show that such an approach is possible. For comparison, in Fig. 7b we present a grid a priori unsuitable for calculation, where the grid's lines go beyond the boundary. It is generated by the standard Winslow method.

Another way to get rid of cells that are not convex using without having to change the grid's dimensionality is by the variational barrier method [7] and its further modifications [28, 29]. Since the algebraic equations of the variational barrier method are the approximation of the same Eqs. (2) as the algebraic equations in the Winslow method, it is sufficient to perform the main calculations for a number (that is not high) of cells near the boundary's breaking point. As a result the computation intensity is not high.

From grid 241×241 for $p = 0.77$ (see Fig. 7a), it is easy to generate a grid consisting of convex cells even with the help of a simple algorithm, which is used as a preliminary stage for the variational barrier method [7] (for more efficient and reliable algorithms see [28, 29]). A certain value $\varepsilon > 0$ is set and by the gradient-search method the following function is minimized $\sum_i\sum_j\sum_{k=1}^{4}[\max(\varepsilon - s_k, 0)]^2$. Here, a summarizing procedure is performed over all the grid's cells, and inside the cell summarizing is performed over its vertices, and s_k is the square of the triangle which is supported onto vertex k. Practically, the summarizing procedure is performed only over those triangles for which $s_k < \varepsilon$.

Figure 8a depicts the grid consisting of convex cells generated from the grid presented in Fig. 7 under $\varepsilon = 10^{-6}$ after 40 iterations. In all iterations a very small number of cells near the corner's vertex A are used.

If it is necessary, it is possible to further improve the grid by using the main stage of the variational barrier method. The result is presented in Fig. 8b. For this grid the minimal square of the triangle is higher approximately by a factor of 7 than it is for the grid presented in Fig. 8a. The economical variant of method [30] is used. In this case for each iteration the main calculations are performed for that set of cells for which the relative misalignment of the algebraic equations that generate the grid is higher than a certain given value. As a result, the summary efforts for 52 iterations needed for generating the grid presented in Fig. 8b corresponds to one iteration of the method for all cells.

4. CONCLUSIONS

For investigating the known problem on generating a regular grid by the Winslow method in a rectangular domain with a boundary kink (corner), a highly accurate numerical method for the inverse harmonic mapping of the unit square onto the domain with a certain mapping of the domain boundaries is developed. The behavior of mapping level lines that enter the point of the boundary kink is studied. Near the kink, the angle between the boundary and the straight line connecting a point on the level line with the point of the boundary kink is found as the function of the coordinate of the point on the level line in the unit square. It is shown that the level line of the mapping is tangential to the boundary at the kink point. Near the kink point the mapping is not quasi-isometric. The regular grid generated according to the intersection points between the level lines connected by straight lines contains a self-intersecting cell that remains when the grid step along the boundary decreases. Based on the universal elliptical equations reproducing any nondegenerate mapping of the parametric rectangle onto a given domain, a simple two-parametric control for grid nodes in the corner is suggested, which makes it possible to control effectively the slope angle of the grid line entering the point of the kink, thereby removing the escape of the grid lines from the domain boundary. In the case of a small number of grid points (31×31), a nondegenerate grid is generated by selecting a suitable value of one parameter. If the number of a grid's nodes is increased by a factor of 8 in both direction (a 241×241 grid), nonconvex cells appear within the domain which are easily removed by using the variational barrier method. Another way of avoiding nonconvex cells is to decrease the grid dimension along the second direction (a 241×121 grid).

ACKNOWLEDGMENTS

I thank O.V. Ushakova, who placed the manuscript and codes at my disposal and made useful comments on the presented paper, and V.I. Vlasov from the Dorodnicyn Computing Center of the Russian Academy of Sciences for criticism.

REFERENCES

1. B. N. Azarenok, "Constructing the grid orthogonal and having the given nodal clustering near the boundary of a twodimensional domain," Math. Models Comput. Simul. **3**, 637 (2011).
2. A. M. Winslow, "Numerical solution of quasilinear poisson equation in nonuniform triangle mesh," J. Comput. Phys. **1**, 149–172 (1967).
3. T. Radó, "Aufgabe 41, Jahresber," Deutsche Math.-Verein **35**, 49 (1926).
4. H. Kneser, "Lösung Der Aufgabe 41, Jahresber," Deutsche Math.-Verein **35**, 123–124 (1926).
5. G. Choquet, "Sur un type de transformation analytique généralisant la représentation conforme et définie au moyen de fonctions harmoniques," Bull. Sci. Math. **69**, 156–165 (1945).
6. S. K. Godunov, A. V. Zabpodin, M. Ya. Ivanov, A. M. Kraiko, and G. P. Prokopov, *Numerical Solution of Gas Dynamics Multidimensional Problems* (Nauka, Moscow, 1976) [in Russian].
7. S. A. Ivanenko and A. A. Charakhch'yan, "Algorithm for generation of curvilinear grids of convex quadrilaterals," Dokl. Akad. Nauk SSSR **295**, 280–283 (1987).
8. S. A. Ivanenko, "Variational methods for adaptive grid generation," Comput. Math. Math. Phys. **43**, 793 (2003).
9. B. N. Azarenok, "Variational method for hexahedral grid generation with control metric," Math. Models Comput. Simul. **1**, 573 (2009).
10. S. A. Ivanenko, "Existence of equations describing the classes of nondegenerate curvilinear coordinates in arbitrary domains," Comput. Math. Math. Phys. **42**, 43 (2002).
11. G. P. Prokopov, "Universal variation functionals for two-dimensional grids generation," Preprint IPM RAN No. 1 (Inst. Prikl. Matem. RAN, Moscow, 2001).
12. S. K. Godunov and G. P. Prokopov, "On the computation of conformal transformations and the construction of difference meshes," USSR Comput. Math. Math. Phys. **7** (5), 89–124 (1967).
13. G. P. Prokopov, "Variational methods of two-dimensional grids calculation in solution of non-stationary problems," Preprint IPM RAN No. 4 (Inst. Prikl. Matem. RAN, Moscow, 2003).
14. G. P. Prokopov, "Realization of variational approach to calculation of two-dimensional grids in unsteady problems," Preprint IPM RAN No. 116 (Inst. Prikl. Matem. RAN, Moscow, 2005).
15. G. P. Prokopov, "Selection of parameters during variational approach to calculation of regular grids," Preprint IPM RAN No. 14 (Inst. Prikl. Matem. RAN, Moscow, 2006).
16. B. N. Azarenok, "Generation of structured difference drids in two-dimensional nonconvex domains using mappings," Comput. Math. Math. Phys. **49**, 797 (2009).
17. P. Knupp and R. Luczak, "Truncation error in grid generation: a case study," Numeric. Methods Partial Differ. Equations **11**, 561–571 (1995).

18. P. Knupp and S. Steinberg, *Fundamentals of Grid Generation* (CRC Press, Boca Raton, FL, 1993).
19. S. A. Ivanenko, *Adaptive-Harmonic Grids* (Vychisl. Tsentr RAN, Moscow, 1997) [in Russian].
20. M. A. Lavrent'ev and B. V. Shabat, *Methods of Complex Variable Function Theory* (Nauka, Moscow, 1987) [in Russian].
21. W. Koppenfels and F. Stallmann, *Praxis der konformen Abbildung* (Springer, Berlin, 1959; Inostr. Liter., Moscow, 1963).
22. E. Yahnke, F. Emde, and F. Lösch, *Tables of Higher Functions* (McGraw-Hill, New York, 1960; Nauka, Moscow, 1977).
23. G. Bateman and A. Erdelyi, *Higher Transcendental Functions* (McGraw-Hill, New York, 1953; Fizmatgiz, Moscow, 1965).
24. V. V. Vecheslavov and V. I. Kokoulin, "Determination of the parameters of the conformal mapping of simply connected polygonal regions," USSR Comp. Math. Math. Phys. **13**, 57–65 (1974).
25. G. P. Prokopov, "About organization of comparison of algorithms and programs for 2D regular difference mesh construction," Vopr. At. Nauki Tekh., Ser. Mat. Model. Fiz. Processov, No. 3, 98–108 (1989).
26. S. I. Bezrodnykh and V. I. Vlasov, "On a problem of the constructive theory of harmonic mappings," J. Math. Sci. **201**, 705 (2014).
27. S. A. Ivanenko, "Control of cell shapes in the course of grid generation," Comput. Math. Math. Phys. **40**, 1596 (2000).
28. S. A. Ivanenko, "Generation of non-degenerate meshes," USSR Comput. Math. Math. Phys. **28** (5), 141 (1988).
29. V. A. Garanzha and I. E. Kaporin, "Regularization of the barrier variational method of grid generation," Comput. Math. Math. Phys. **39**, 1426 (1999).
30. A. A. Charakhch'yan, "An approach to reducing the computational cost of constructing curvilinear grids," Comput. Math. Math. Phys. **38**, 333 (1998).

Translated by Yu.V. Zikeeva